ThermoFisher SCIENTIFIC

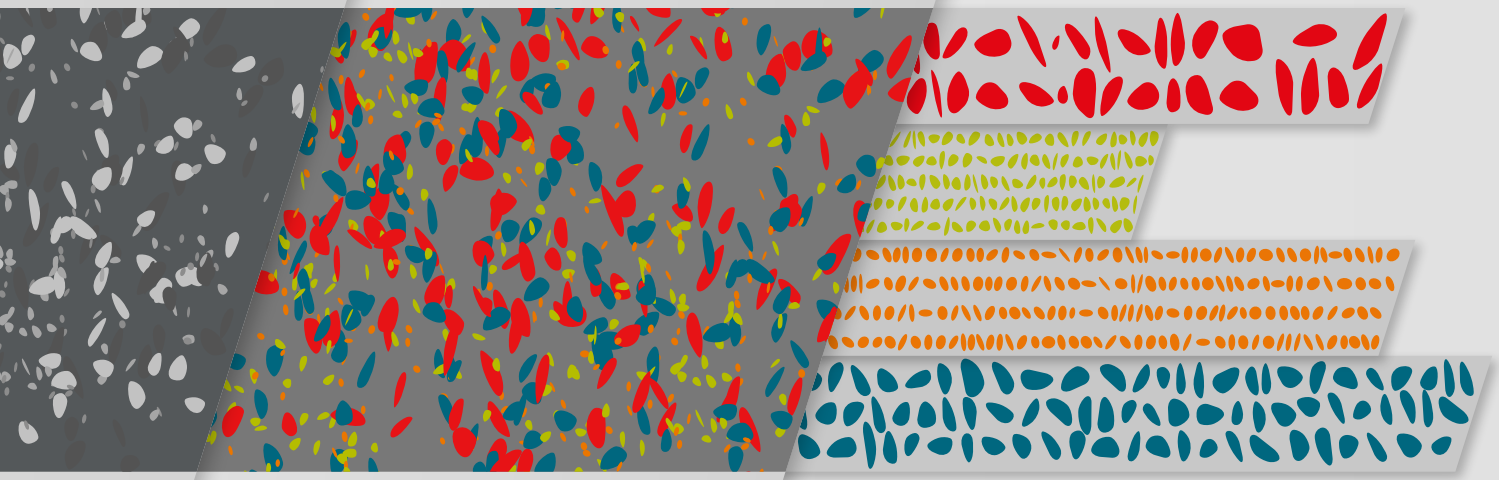

APW – Automated Particle Workflow

Unlocking high-throughput, reproducible nanomaterials characterization with TEM

thermo scientific

Transmission electron microscopy (TEM) is an established technique for nanomaterial characterization, capable of providing precise, high-resolution imaging, as well as detailed structural and chemical information, at the atomic scale. This makes TEM an excellent tool for the study of materials, especially when nanoscale insights are needed. However, traditional TEM analysis is often limited by its complexity, low throughput over long timespans, and high risk of user bias during both image acquisition and post-processing. This hinders the reproducibility and efficiency necessary for large-scale quantitative studies.

Automated workflows have been increasingly used to overcome these limitations. The Thermo Scientific™ Automated Particle Workflow (APW) integrates Thermo Scientific™ Velox™, Maps, and Avizo™ 2D Software into a comprehensive end-to-end solution for TEM and scanning TEM (STEM) analysis (Figure 1).

Velox and Maps Software facilitate automated, large-area, multi-signal data acquisition (as in TEM/STEM imaging with energy-dispersive X-ray spectroscopy (EDS) mapping), which significantly reduces user-biased intervention during data collection.

Once acquired, the raw datasets can be seamlessly evaluated with Avizo 2D Software, which is capable of performing image segmentation, quantitative analysis, and has the option to implement machine learning algorithms for specialized or challenging use cases. Avizo 2D Software allows dataset export in multiple formats (such as .csv), which can then be further processed as needed.

APW combines automated stage control, high-throughput imaging, and intelligent image analysis for the efficient, reproducible, and statistically robust characterization of large nanoparticle populations, or low-concentration features over wide sample areas.

This results in accelerated quantitative analysis and helps ensure high reproducibility, with comparable results across multiple experiments. By streamlining the entire characterization pipeline, APW sets a new standard for high-throughput, quantitative TEM analysis of nanomaterials.

APW is well suited for a range of nanomaterial applications such as quality control in nanoparticle synthesis (assessing size distribution as well as agglomeration behavior), precipitate statistics in alloy systems (evaluating volume fraction and elemental composition), defect analysis in metals (identifying dislocations and grain boundaries), etc. A series of illustrative applications are presented in this eBook, showcasing the efficiency and accuracy of APW.

Velox Software
An integrated platform for both TEM and STEM experiments offering fast and efficient multichannel data acquisition and analysis.

Maps Software
An automated platform for multi-scale imaging offering stitched large-area tiled images from overviews down to full resolution.

Avizo 2D Software
A powerful platform for 2D visualization and analysis supporting everything from particle segmentation to AI driven automated workflows.

Figure 1. APW combines Thermo Scientific Velox and Maps Software (for rapid, large-area multi-channel acquisition) together with Thermo Scientific Avizo 2D Software (for particle segmentation and classification). This integrated workflow enables unattended batch processing, quantitative particle analysis, and provides clear visual graphs for nanomaterial studies.

Accelerating statistical analysis of core-shell nanoparticles

The unique structure of core-shell nanoparticles (NPs) makes them highly valuable across multiple fields, offering a customizable platform where properties such as stability, reactivity, and functionality can be tightly controlled. Core-shell NPs play critical roles in catalysis, drug delivery, energy storage, and sensing. Additionally, in energy technologies such as batteries and fuel cells, core-shell NPs can improve electrochemical performance by enhancing ion transport while minimizing undesirable side reactions.

Obtaining statistically meaningful insights from core-shell NPs requires the analysis of large sample areas, which is particularly challenging due to the slow and often biased nature of conventional manual segmentation. Therefore, analysis is typically limited to just a few hundred particles, which may not be enough to truly represent the characteristics of the whole sample.

APW overcomes these limitations by delivering high-throughput, unattended characterization of core-shell NPs. Through a combination of Velox and Maps Software, the workflow can acquire and stitch together large arrays of images into sample maps.

Figure 1.1 shows an example of this mapping for core-shell NPs using a 28-tile HAADF-STEM array. It is common to set the tile overlap in these maps to a certain percentage in order to compensate for small inaccuracies caused by the stage movement. In this example, 20% of each tile is set.

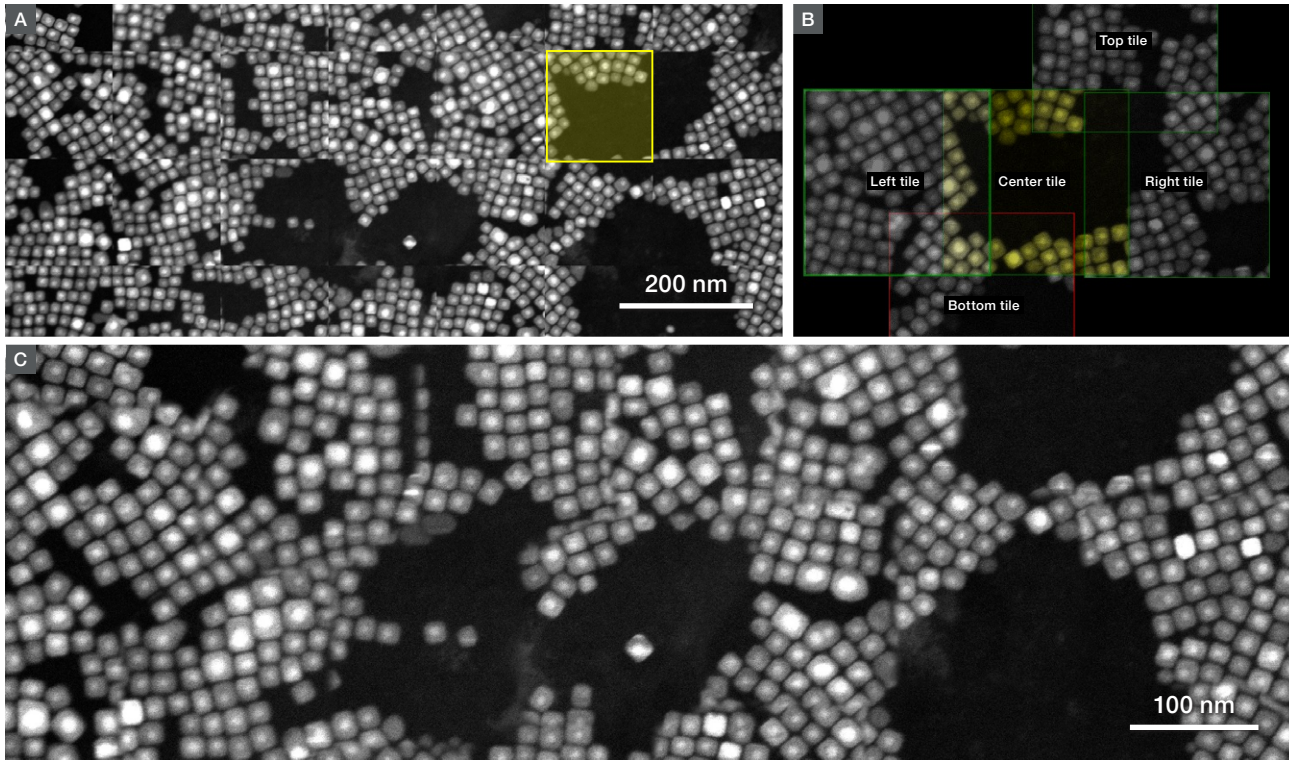

Figure 1.1. A) Unstitched set of 28 individual HAADF-STEM image tiles collected for a core-shell NP sample. B) Automatic alignment and stitching of tiles into one seamless composite image with Maps Software. C) Resulting overview showing a continuous, large-area representation of the sample, which enables comprehensive structural analysis. *Sample courtesy of Dr. Damien Hudry and Prof. Bryce Richards, Karlsruhe Institute of Technology, Germany.*

Once the tile image acquisition is complete, Avizo 2D Software is used to directly segment the acquired dataset, providing real-time particle statistics such as size, core diameter, surface area, and perimeter (Figure 1.2). The entire fully unattended workflow ran in just 1.5 hours, delivering statistical data for ~1,500 particles; this is a much higher efficiency than would be possible with traditional, manual methods.

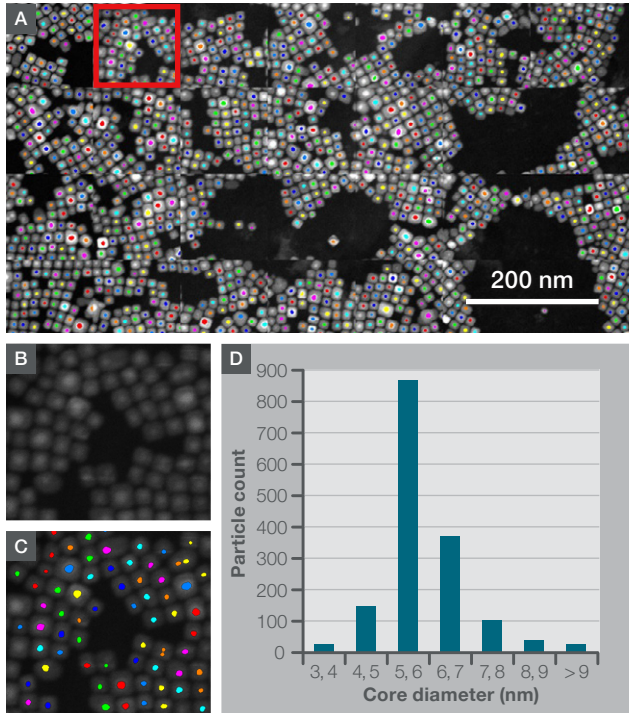

Figure 1.2. A) Core segmentation with Avizo 2D Software of the 28-tile HAADF-STEM array shown in Figure 1.1 (1,548 cores were identified). B-C) Close ups of a single tile (marked with a red square in A) and its core segmentation. D) Histogram showing the size distribution of cores, indicating that ~80% of the cores fall between 5–7 nm.

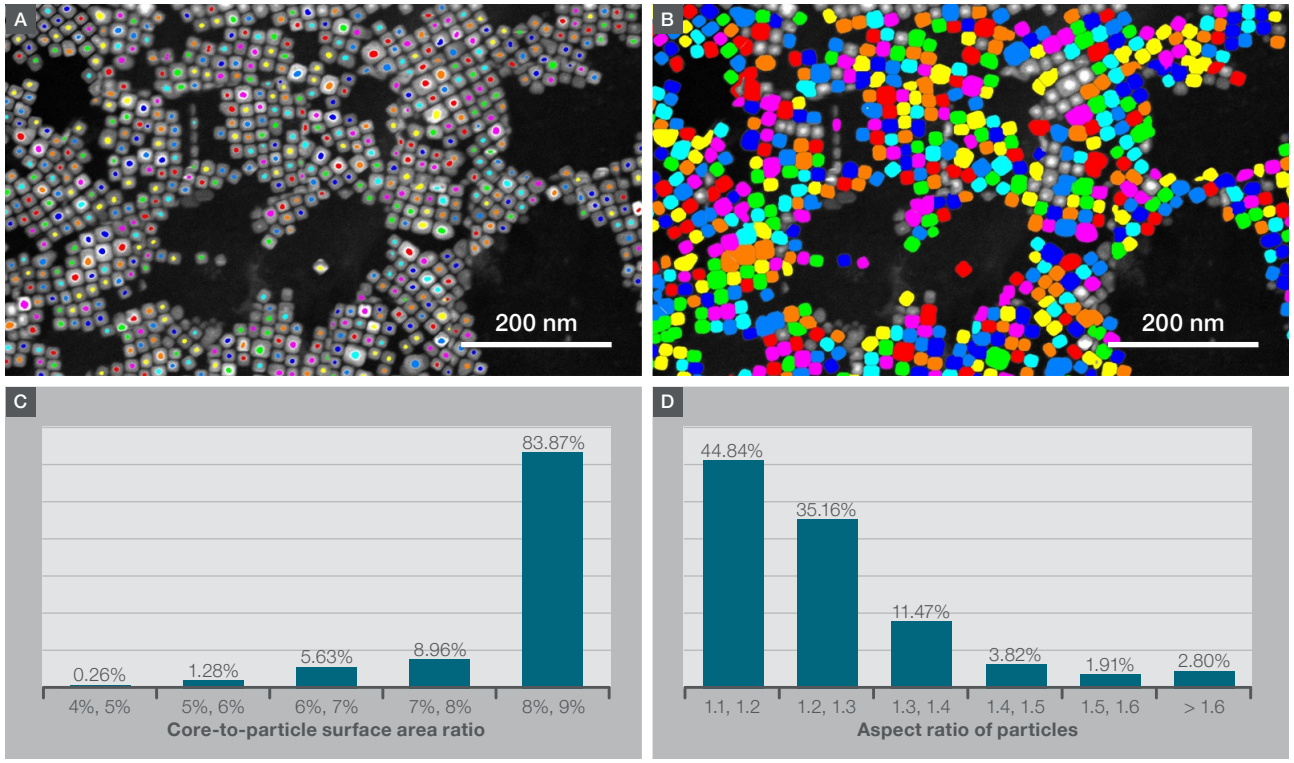

Figure 1.3. Core (A) and whole-particle (B) segmentation of the stitched overview (post-processing video). C) Surface area ratio between cores and particle; ~93% fall between 7-9%, indicating shell-rich core-shell NPs. D) Length/width ratio of particles; ~80% are ≤1.3, indicating that a majority have a quasi-square shape.

As mentioned previously, each individual tile has 20% overlap with its neighbors, meaning that many of the nanoparticles are being counted multiple times. In order to obtain reliable characterization, statistics should therefore be derived from the stitched overview. As shown in Figure 1.3, only ~855 cores are identified in the stitched overview, or about 55% of the overall count obtained from the 28 unstitched tiles.

Post-processing of the acquired dataset with Maps and Avizo 2D Software can reveal further statistical insights. For example, segmentation of whole particles is shown in Figure 1.3A; 785 particles were analyzed, showing that >90% cores are successfully encapsulated within shells (a similar value can be obtained from the unstitched tiles as well). The uniformity of the NPs can also be determined by analyzing the particle aspect ratio (length/width), or the ratio of the core to particle surface area (obtained by matching the coordination of cores and particles in the software).

Monitoring heat-treatment-induced changes in the shape and size of Mn precipitates within an Al alloy

Manganese is a common precipitate doped into aluminum alloys to improve mechanical, corrosion, and thermal stability. The size, morphology, and structure of the precipitates strongly influence their strengthening behavior as well as long-term performance.

Understanding and tailoring these micro- and nano-structures is therefore essential in order to optimize process parameters and to obtain desired performance. The shape and size distribution of the Mn precipitates can be fine-tuned by post-heating. To optimize the parameter of this process, precipitates must be examined before and after heat treatment, thereby assessing whether the process drives the desired morphological changes.

One of the main challenges in the analysis of Mn precipitates is their identification and segmentation, which is hampered by the non-uniform substrate, the varying contrast of the Mn precipitates with respect to the background, as well as other precipitates/impurities with similar contrast (these have been highlighted separately in the bright field image shown in Figure 2.1).

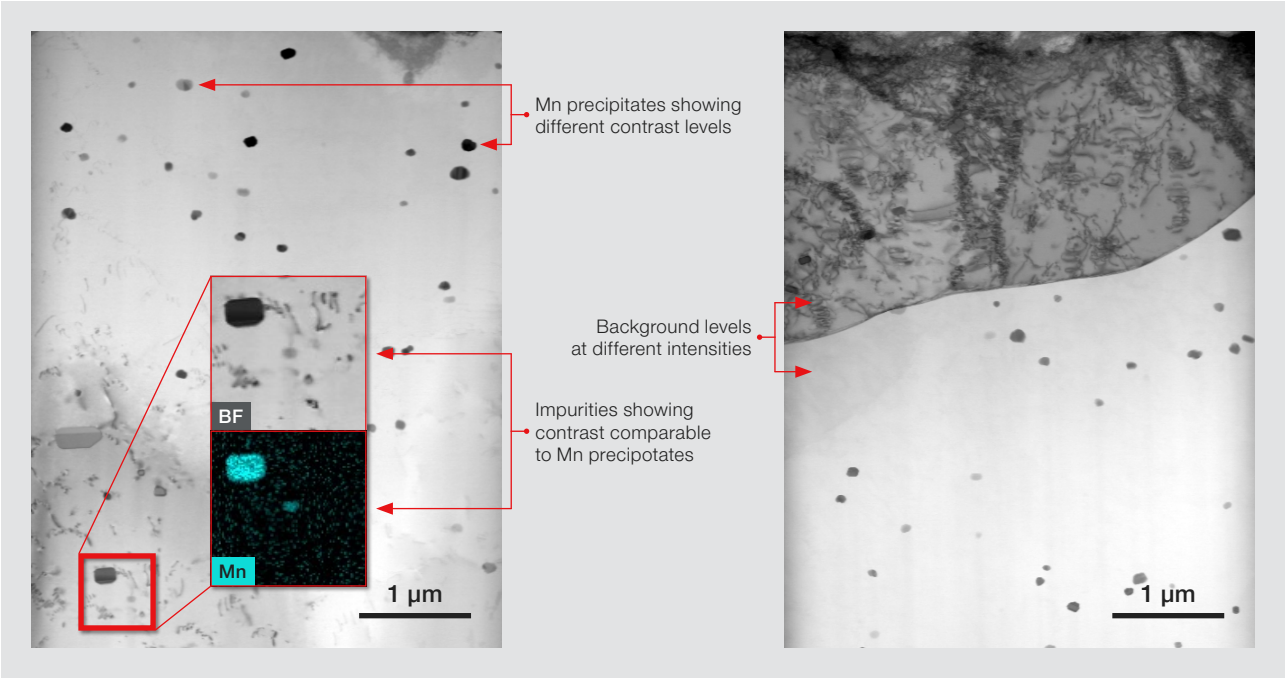

Figure 2.1. Mn precipitates in an Al alloy before (left) and after (right) heat treatment. Labels indicate some of the complicating factors that can impact the identification of the precipitates using only bright field (BF) imaging. The surface background, the contrast of the precipitates themselves, and the contrast of comparable impurities all hinder accurate segmentation. ***Sample courtesy of Daniel Chrast and Dr. Stepan Kolomy, Frencken Group Limited, Netherlands, and Brno University of Technology, Czechia.***

To identify only Mn precipitate accurately, a combination of TEM/STEM imaging and EDS mapping is required. Velox Software enables simultaneous acquisition of multichannel data, including structural and compositional information, providing correlative observations that reveal particle size, morphology, and elemental composition.

These datasets can be collected automatically by linking Maps and Velox Software. The tiles are then stitched with Maps Software and subsequently analyzed with Avizo 2D Software.

EDS mapping and TEM imaging provide valuable complementary information, as is shown in Figure 2.2. The Mn EDS map can be used to accurately locate and mark the position of the Mn precipitates, effectively excluding impurities with similar contrast while also identifying precipitates that are otherwise obscured by the surface background. While highly valuable, EDS mapping has difficulty providing precise morphological or structural details, particularly when acquisition time is limited. Bright-field TEM imaging, meanwhile, can be used to accurately analyze the shape and size of the precipitates. The combination of these methods, therefore, makes segmentation and characterization far more reliable and precise.

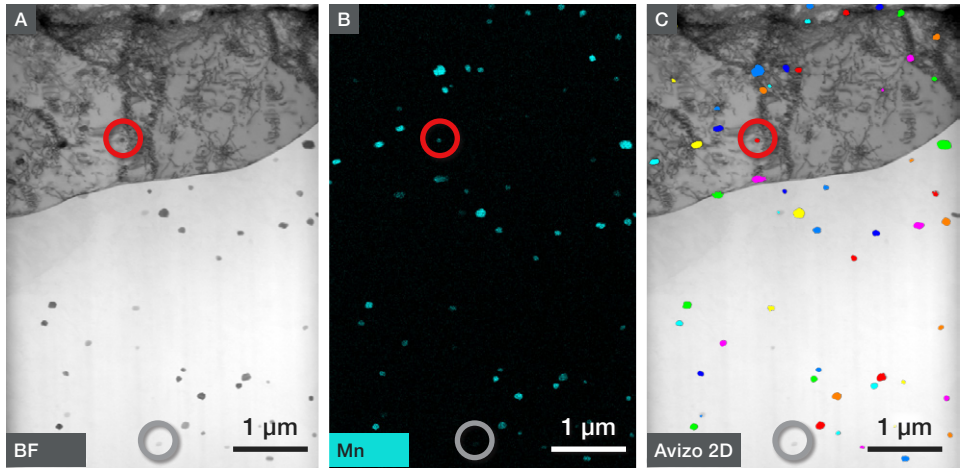

Figure 2.2. Advantages of combined bright field TEM imaging and EDS elemental mapping in the analysis of Mn precipitates within an Al alloy. BF imaging (A) reveals high-resolution morphological detail while the EDS map (B) localizes Mn precipitates, excluding impurities and background artifacts. This correlative approach enables more robust and precise segmentation of the Mn precipitates (C). The top red circles showcase how EDS data can identify and segment Mn precipitates that are otherwise obscured by the background contrast. The bottom grey circles highlight how EDS can also help exclude precipitate that are not Mn. Note that any precipitates that fall across the border of the image were excluded from the analysis in order to obtain more accurate size and shape distributions.

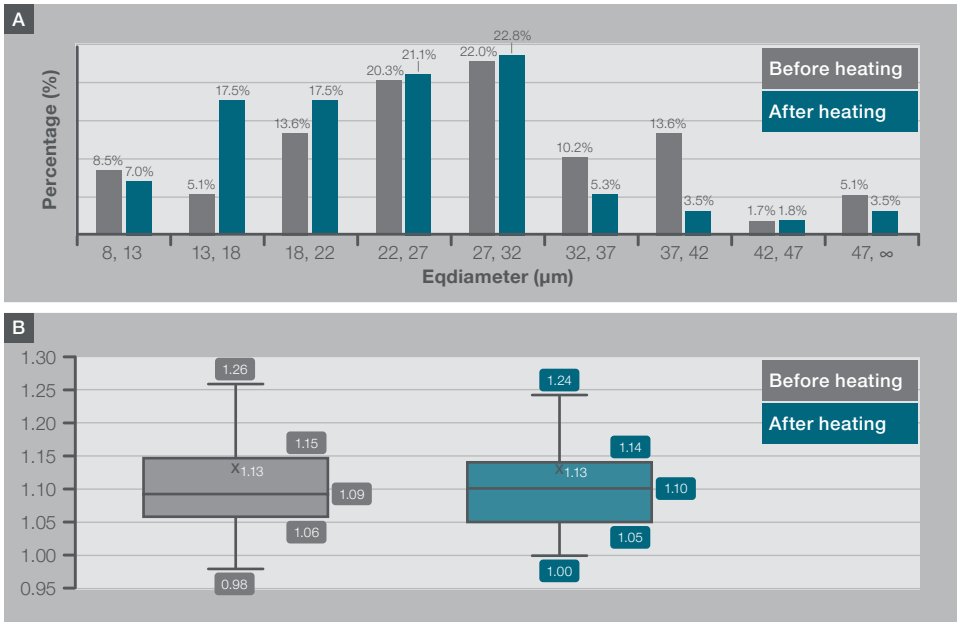

Figure 2.3. A) Statistical overview of Mn precipitates, obtained using a .csv data export from Avizo 2D Software. Clear changes after heating can be seen, with a shift towards smaller particles in the size distribution chart. B) Graph quantifies roundness, with 1 indicating a perfect circle. This parameter remained largely unchanged after heating, with a slight reduction in the interquartile range. This likely indicates an improvement in shape uniformity and a slight trend toward more spherical precipitates after heating. Note that outliers are not shown, for clarity.

As demonstrated in the previous example, a statistical overview of particle properties can be obtained with Avizo 2D Software. Here, the size and shape of the Mn precipitates were examined before and after heating using a .csv export. The sorted data shows that the heating process modifies the morphology of the Mn precipitates, as indicated by an overall decrease in size. Specifically, 42.0% of Mn precipitates are smaller than 22 µm after heating, compared with 27.2% before heating; conversely, the fraction of large precipitates (>32 µm) decreases from 30.6% to 8.8% (Figure 2.3). The roundness of the Mn precipitates is quantified by Shape_AP, a direct metric in Avizo 2D Software, where 1 corresponds to a perfect circle, and deviations indicate reduced sphericity. As seen in Figure 2.3, heating does not significantly alter precipitate roundness. However, the slightly narrower interquartile range and reduced box body width suggest that the variation in shape becomes slightly more constrained, indicating a modest improvement in the overall spherical shape uniformity of Mn precipitates after heating.

Automated segmentation and statistical analysis of a single precipitate type during multichannel acquisition

In advanced electron microscopy, researchers often need multiple imaging and analysis channels to obtain comprehensive sample information (e.g., bright field and dark field imaging along with EDS of certain elements).

While multichannel acquisition provides rich datasets, it also increases the complexity of the subsequent analysis. In this example, automation is used to address the challenges of such data acquisition, quantification, and segmentation for a single precipitate type within a heterogeneous matrix. The specimen is an Al-Cu-Li alloy (2055), which is widely used in the aerospace industry for its low weight and excellent mechanical properties. The use of several EDS channels was critical for the identification of specific precipitate types (mainly Mn and Zr) against the non-uniform background. The type, morphology, and distribution of these precipitates strongly influence the alloy's deformation behavior, and these properties are dependent on both heat treatment and alloying conditions.

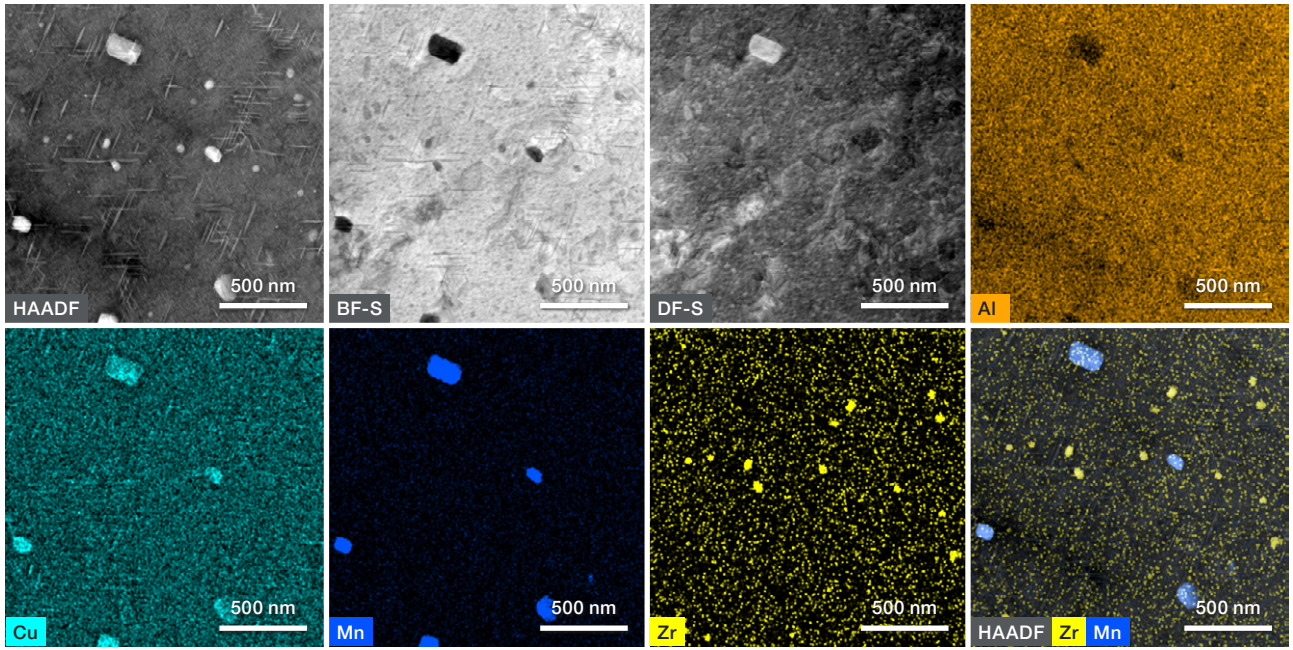

Figure 3.1. Multichannel electron microscopy of an Al-Cu-Li (2055) alloy, including HAADF, BF, and DF imaging along with EDS maps of Al, Cu, Mn, and Zr. The combined data enables the differentiation of Mn- and Zr-rich precipitates from the background matrix. The whole dataset was acquired simultaneously with Velox Software. ***Sample courtesy of Michal Jambor, Czech Academy of Sciences, Czechia.***

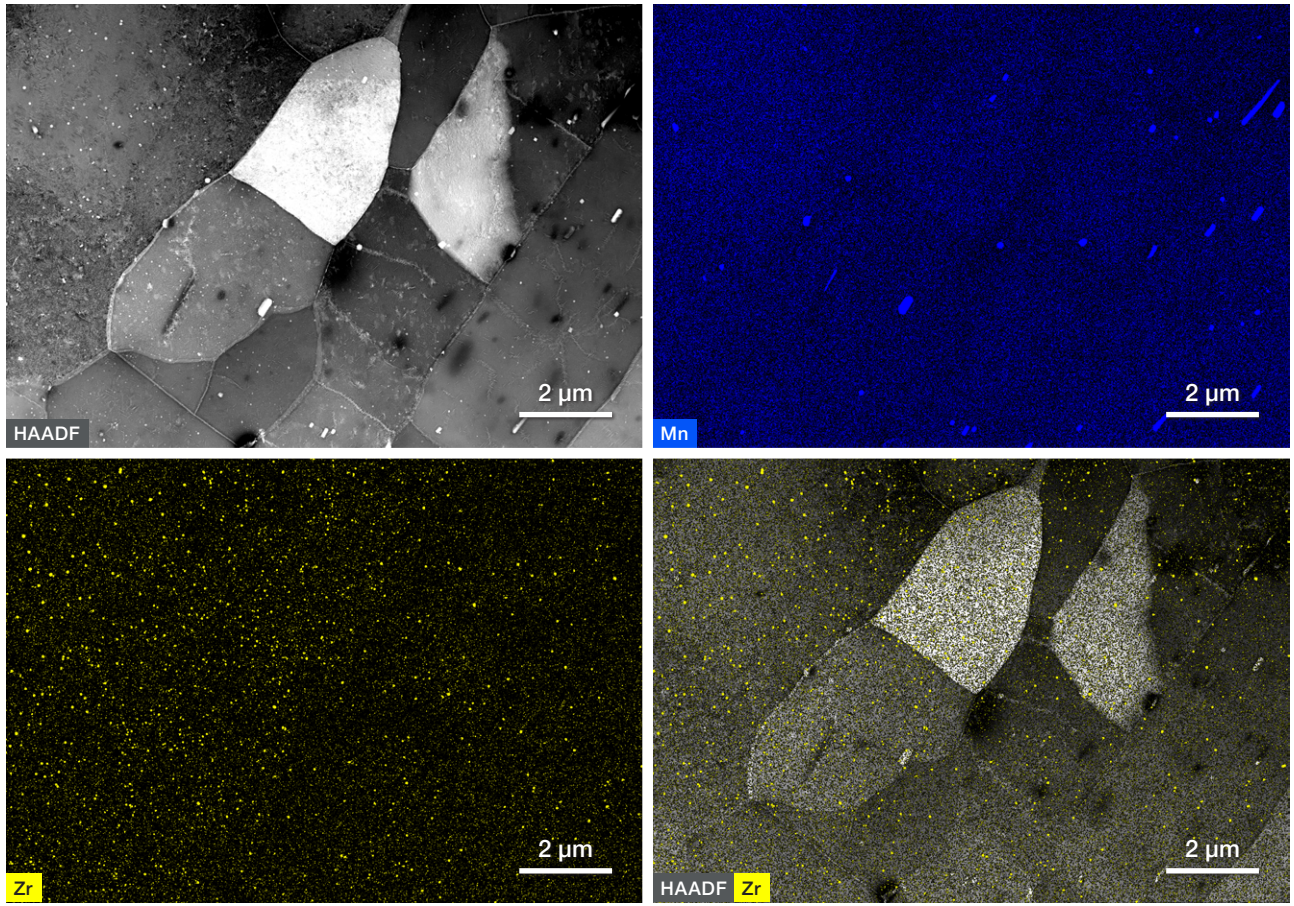

Figure 3.2. Stitched 48-tile overview of an Al-Cu-Li alloy, showing HAADF imaging, EDS maps of Mn and Zr, as well as an overlay of HAADF imaging with Zr mapping. A segmentation recipe in Avizo 2D Software was used to selectively view the chosen channels for automated single-precipitate segmentation during the multichannel acquisition.

A stitched 48-tile overview was created in Maps Software to perform statistically meaningful characterization of precipitate size and shape distribution. Figure 3.2 shows two stitched overviews highlighting either Mn-rich or Zr-rich precipitates. Mn-rich precipitates are relatively large and sparsely distributed; as a result, they could still be analyzed using traditional manual segmentation. Zr-rich precipitates, meanwhile, are much smaller and more densely distributed, making APW a more suitable solution, as it can efficiently process these large datasets. Within APW, the built-in segmentation recipes in Avizo 2D Software can be configured to use only selected channels, enabling automated single-precipitate segmentation and analysis during multichannel acquisition. This approach represents a critical step toward high-throughput materials characterization, which can ultimately accelerate process optimization and improve material performance.

An unstitched 48-tile overview of the alloy shows the precipitate distribution across a large sample area (Figure 3.3). A close-up view of the first HAADF tile, along with the corresponding segmentation in Avizo Software, highlights how individual Zr-rich precipitates can be distinguished, even within precipitate-dense regions. Statistical analysis of the stitched overview reveals that most Zr-rich precipitates have an area below 2,000 nm^2, with only a minor fraction exceeding 3,000 nm^2. Elongation analysis indicates that approximately 42% of the Zr-rich precipitates exhibit elongation values between 0.6 and 0.8, suggesting a moderately anisotropic morphology instead of an equiaxial shape. Together, these quantitative results demonstrate how large-area multichannel mapping, combined with automated segmentation, enables not only efficient data acquisition but also reliable statistical characterization of precipitate populations.

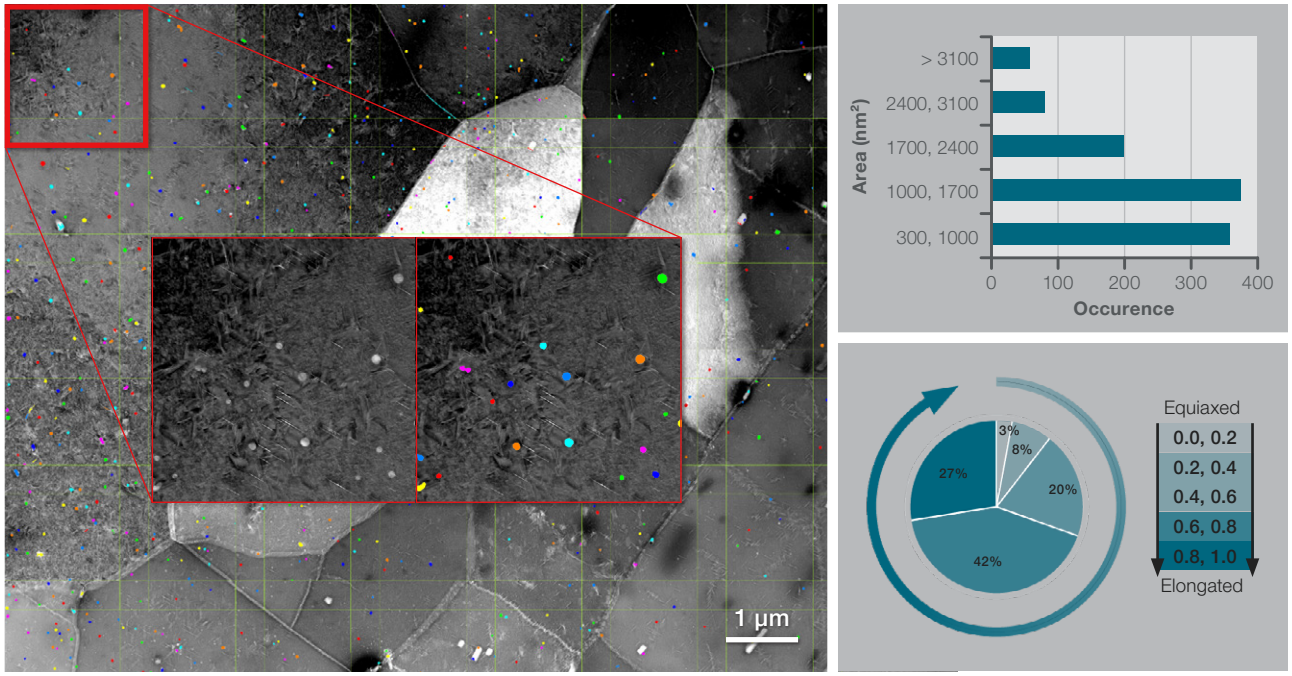

Figure 3.3. Large-area 48-tile overview of an Al-Cu-Li (2055) alloy, highlighting Zr-rich precipitates. The close-up shows a single HAADF tile along with the corresponding segmentation in Avizo Software. Statistical analysis of the stitched dataset reveals that most Zr-rich precipitates have an area below 2,000 nm^2. Elongation statistics further show that ~42% of precipitates fall within a range of 0.6–0.8, indicating moderately anisotropic morphologies. This combined mapping and segmentation workflow enables efficient large-scale characterization and quantitative analysis of precipitate populations.

Conclusions

The Automated Particle Workflow is a comprehensive solution designed to bring automated electron microscopy to a variety of nanostructural analyses. By integrating advanced imaging, multichannel data acquisition, and automated particle characterization, APW can provide a significant increase in sample coverage compared to manual methods without compromising data quality or statistical reliability.

The workflow streamlines the entire process from unattended image acquisition and particle segmentation to automated EDS analysis and statistical data export. This minimizes operator bias and helps to ensure reproducibility, transforming heavily operator-dependent tasks into an automated solution that generates large, statistically meaningful datasets.

This capability helps provide deeper insights into material behavior, accelerates discovery cycles, and enables more confident decision-making in both academic research and industrial applications.

ThermoFisher SCIENTIFIC

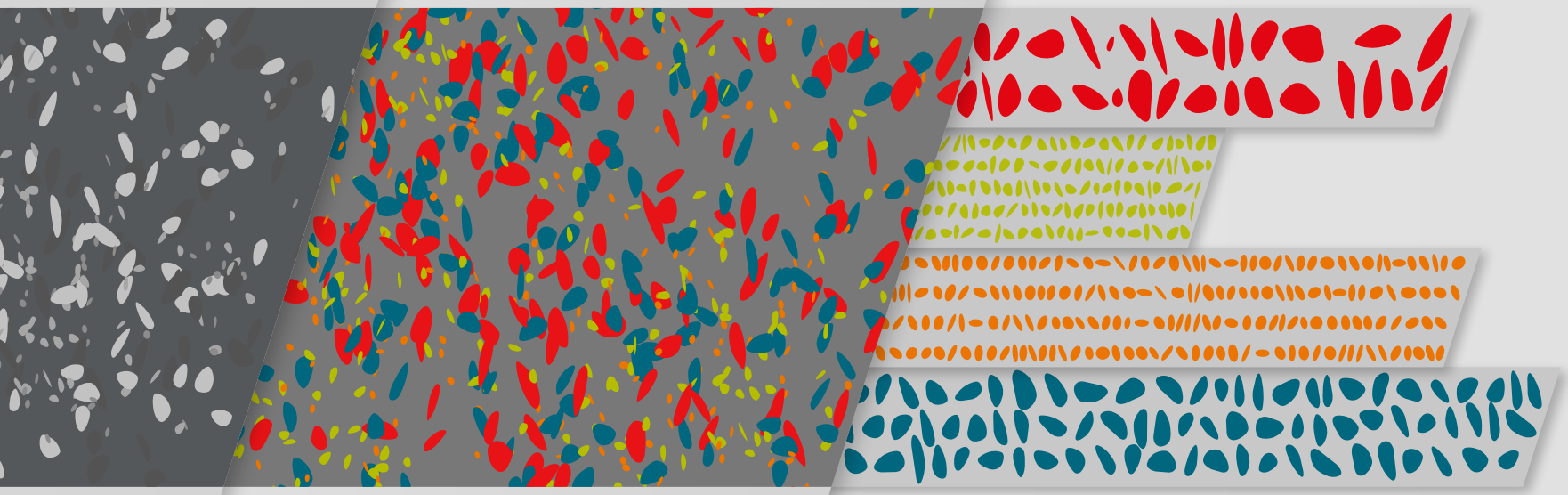

Learn more at **thermofisher.com/apw**

thermo scientific